FUDMA Journal of Sciences (FJS)
ISSN online: 2616-1370
ISSN print: 2645 - 2944
Vol. 4 No. 4, December, 2020, pp 67 – 76
DOI: https://doi.org/10.33003/fjs-2020-0404-408

PHOTOCATALYTIC OPTIMIZATION OF MR DYE BY K-ZnO AND ZnO CATALYSTS UNDER VISIBLE IRRADIATION

[*1]Yusuf Ibrahim, [1]Yusuf Usman Jibrin, [1]Zaharadden Muhammed and [2]Mujahid Abubakar

[1]Department of Chemistry, Sule Lamido University Kafin Hausa,
[2]Department of Biological Sciences, Sule Lamido University Kafin Hausa. P.M.B 0038, Jigawa State, Nigeria
Corresponding author: Tel: +2348133376693
E-mail: ibrahimy864@gmail.com

ABSTRACT
The lucubration on the visible light methyl red (MR) degradation using K-ZnO and undoped ZnO photo catalyst was investigated. The successive formation of K-ZnO was ascertained by several techniques such as scanning electron microscopy (SEM), Fourier-transform infrared spectroscopy (FT-IR), and UV-Visible spectrophotometer and solid state UV-Vis band gap energy determination by comparing the Kubelka-Monk equation with Tauc equation and the energy band gap was calculated to be 3.28ev. The influence of reaction variables such as MR concentration, reaction pH, catalyst loadings and temperature have been investigated for both process. The kinetics model was developed for both doped and undoped ZnO photocatalyst using pseudo first and second order kinetics, the result indicated that both doped and undoped ZnO followed pseudo first order kinetics due to higher correlation coefficient (R^2) value of 0.985 and 0.922 with rate constant (k) of 0.026 min^{-1} and 0.062 min^{-1}, respectively. Based on the rate constant value (k) obtained at different reaction temperatures, the Arrhenius expression was derived. The derived activation energy (Ea) for the degradation of MR by K-ZnO photocatalysis was $32.109x10^3 JK^{-1}$. The optimum condition for K-ZnO showed nearly complete degradation (95%) of the dye molecules with slightly higher degradation efficiency compares to ZnO (91%).

Keywords: Methyl red; K-ZnO; Photo catalysis; Kinetics.

INTRODUCTION

Environmental pollution has become the concerns problems and challenges. Large amount of industrial wastewater is generated every year from petrochemical, textile, pharmaceutical, chemical and automotive industries (Wang *et al.*, 2020). Dyes are the most hazardous contaminant especially in the aquatic environment, among them methyl red (MR) which is commonly used as ink jet printing, textile industries, pH indicator in the laboratories and other uses (Omotunde *et al.*, 2018). MR dye usually causes skin, eye and digestive track disturbance if ingested or inhale (Zaheer *et al.*, 2019). Without an effective wastewater treatment process, these seize a high risk to human health affecting the life style of humans and aquatic animals (Egea-Cobacho *et al.*, 2019) (Basavarajappa *et al.*, 2020). Various conventional process have been used for removal of dyes containing wastewater, these methods are biological method (Das and Mishra 2017), filtration methods (Jiang *et al.*, 2018), and chemical methods (Ahmadi *et al.*, 2018) and other alike process. Most of those processes have their own short coming such as production of secondary contaminant, high cost, and difficulty in the process. Advanced oxidation process (AOP's) is the substituent process, which has the ability to degrade almost all the complex organic compounds (Tominaga *et al.*, 2018) and the use of UV/Vis irradiation in combination with metal oxide catalyst (Yu *et al.*, 2019). TiO_2 is the most frequently used photo catalyst due to its wide range of organic compound; ZnO is seen as appropriate option to TiO_2. More over the catalyst ZnO has been found to be more economical due to its low cost than corresponding TiO_2, and possess higher photocatalytic efficiency in some cases; ZnO has attracted impressive attention due to its better electronics, optical and chemical properties with high photosensitivity and its non-toxicity (Bechambi *et al.*, 2015). ZnO is a unique material with band gap 3.37*ev* and large binding excitation energy of 60M*ev* (Gaya *et al.*, 2009). Modification of ZnO properties to increase its photon responsiveness was achieved by doping with metals such Ag, Co, Fe, Zr, Cr and Mo and with non-metals such as N, F, S, C and B that can replace oxygen in the crystal lattice (Liu *et al.*, 2018). In this present study, as-synthesized K-ZnO has been prepared to minimize the rate of electron-hole recombination of the ZnO catalyst in the photon oxidation process. The K-ZnO is expected to show a noticeable efficiency in photocatalytic activity for degradation of MR.

Materials and Methods:

Chemicals:

ZnO (99%) from Analar BDH, KOH (Global Chemie), Methyl red (95% dye content) Sigma Aldrich, NaOH (99.0%), H_2SO_4 (96%) and Acetic acid ($C_2H_4O_2$) from Ideal Scientific, were used as received without further purification.

Preparation of Methyl Red:

100ppm of methyl red (MR) was prepared by adding 0.10g of MR into small amount of distilled water in 1000ml volumetric flask the mixture was shaken until the MR particles dissolved and filled the flask to the mark with water.

Preparation of K-ZnO:

Required amount of Zinc oxide was dissolves in water under stirring condition for 30min, acetic acid (CH_3COOH) was added to prevent the formation of Hydroxides. Required gram of KOH as a Potassium source was added to the above mixture. Then a few drop of 1M NaOH was added for pH adjustment at pH range of 12-13 with continuous vigorous stirring until a viscous white precipitate is produce. Later the solution was transpose in to the Teflon Stainless Steel autoclave which was carefully sealed and retained at 160ºC for the reaction time 5 hours. The final white sample solution were isolated using centrifugal machine at the rate of 800rpm in 20minute and the obtained solid sample was washed several time with ethanol and deionized water and centrifuge to remove an undesirable ions present in the solution. The end product was dried at 80ºC and calcined at 400ºC in 6 hours (Bechambi *et al.*, 2015).

Catalyst Characterizations:

The FT-IR analysis, were performed on a SHIMADZU FT-IR-8400s Fourier-transform Infrared spectrophotometer. Prepared K-ZnO catalyst was filtered washed and dried then subjected to IR analysis using FT-IR Spectra. The infrared were measured from 400 to 4000cm^{-1} at room temperature.
The Morphology of the modified catalyst will be determines by scanning electron microscopy (SEM) (Leica Stereoscan – 440 SEM) Image. Each of the sample catalysts spread on the carbon tape mounted on the SEM stub.

Photocatalytic Experiment:

The photocatalytic experiment was carried out in a well immersion photocatalytic reactor containing 100ml dye solution in which ZnO is suspended in desired concentrations, a 300W halogen tube was used as a light sources. The solutions were continuously magnetically stirred in a dark for at least 30minute to allow equilibrium absorption of the dye molecule on catalyst particles. The solution pH was adjusted to desired level using H_2SO_4 and NaOH. During the reaction experiment 5ml of the sample suspension was removed at different time distances and centrifuge at 3500rpm to remove catalyst particle completely and analyzed using UV-Vis spectrophotometer. Each experiment was repeated three or more times.

Degradation Efficiency:

The electronic spectrum of MR was recorded over a wavelength ranges 380 to 800nm using a Perkin Elmer UV win lab UV-Vis spectrophotometer facility. The absorbance is maximum at wavelength (λ_{max}) of the dye was 410 nm. Therefore, the dye absorbance with reaction time was recorded at λ max = 410 nm and concentrations were calculated with aid of calibration curve. Photo catalytic degradation efficiency of MR was estimated as follows:

$$\%\ Degradation = \left(1 - \frac{C_t}{C_o}\right) X\ 100 \quad \text{..... (1)}$$

Thus; C_o is the initial concentration of MR and C_t is the concentration of MR after time t.

RESULTS AND DISCUSSIONS:

Characterization of Catalysts

Scanning Electron Microscopy (SEM) analysis was introduced to study the morphology of the pure ZnO and K-doped ZnO. The SEM micrograph image (i.e. Figures 1a and 1b) of K-ZnO and ZnO respectively show the high magnification image of high degree uniformity with K^+ deposited on the surface of ZnO. Critical observation of the micrographs reveals that the doped K-ZnO is more compacted than undoped ZnO.

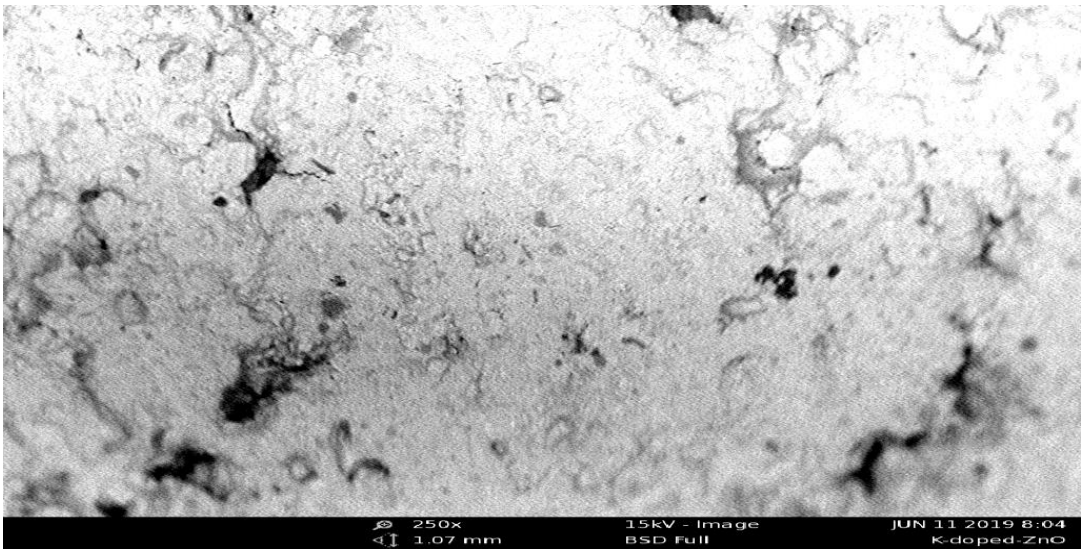

Fig. 1a: SEM image of K-ZnO

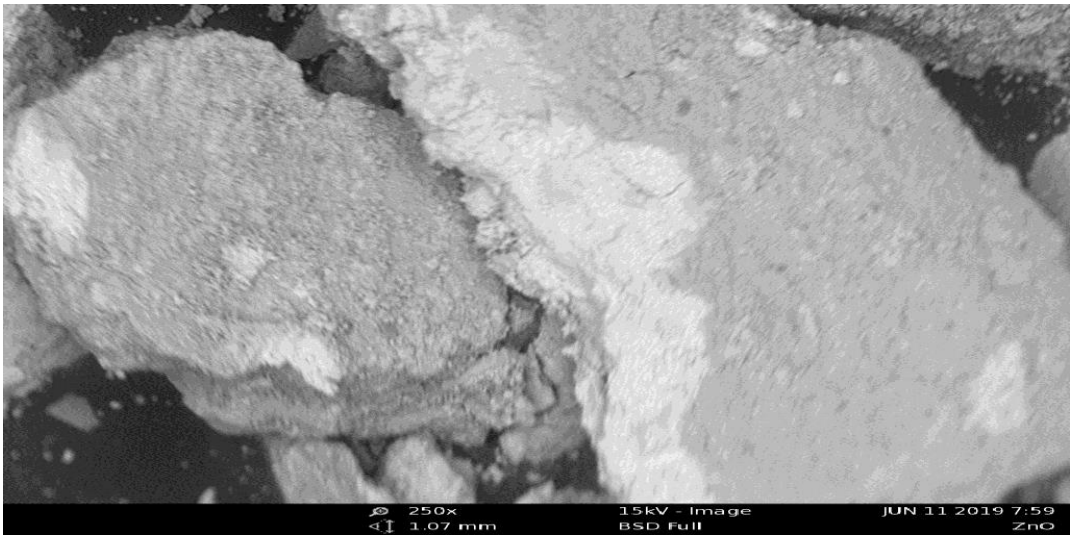

Fig. 1b: SEM image of naked ZnO

Figures 2 and 3 show the FT-IR spectrum of K-ZnO and ZnO respectively, the commercial ZnO recorded at the range of 400-650cm^{-1}, therefore ZnO exhibit their characteristic peaks in this region of 444.61cm^{-1}. The inset shows the FT-IR spectrum was recorded at 400-4000cm^{-1}. The specific single peak at 444.61 cm^{-1} was related to the vibration of Zn and O present due to vibration modes of zinc and oxygen (Prince Richard *et al.,* 2017). And also in the spectrum of K-ZnO, band appears at 3405.44cm^{-1} was due to –OH stretching vibration indicating the present of H_2O originating from the surface of doped catalyst. It can be seen that from the Figure 2 the right shift of the peak to 432.07 was ascribed to Zn-O stretching vibration originating in the doped catalyst which shows that the network of Zn-O-Zn is perturbated by potassium Dopant cited in the lattice (Cheng *et al.,* 2019). The characteristic peak found at 432.07cm^{-1} is the vibration of K-O present in the K-ZnO catalyst.

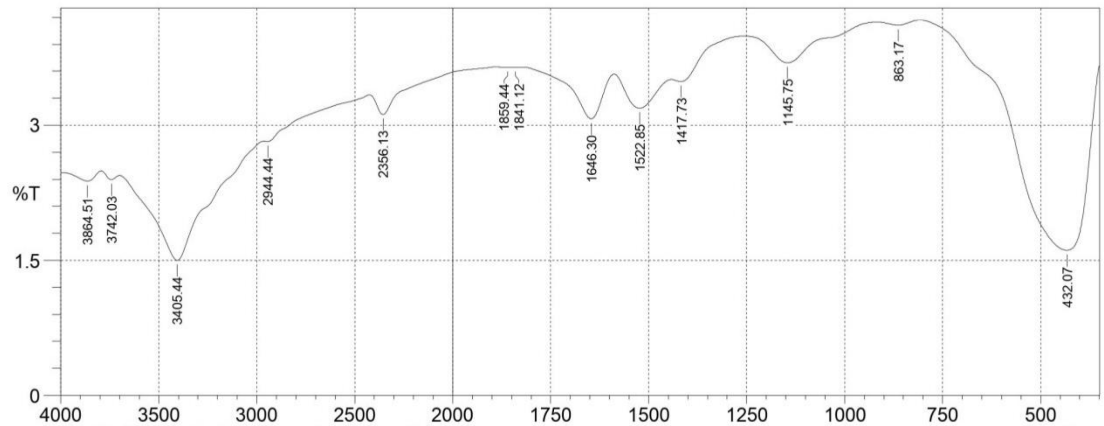

Fig. 2: FT-IR spectrum of K-ZnO

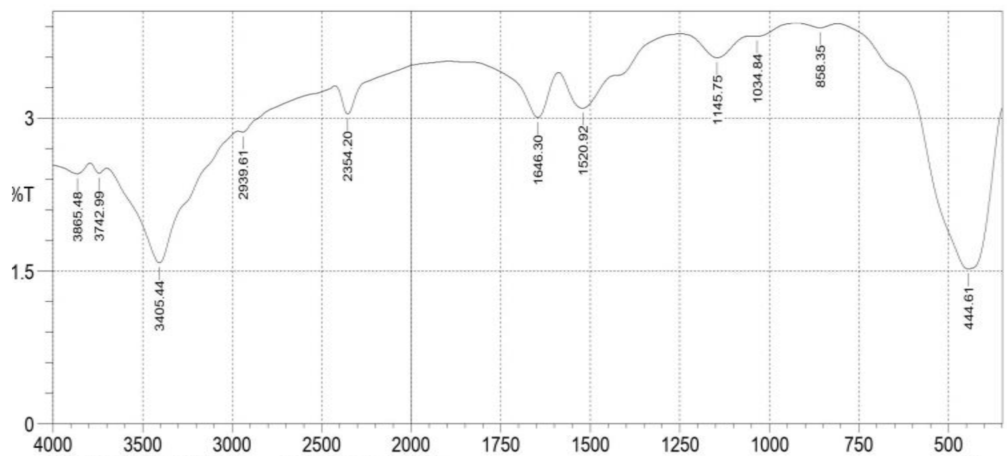

Fig. 3: FT-IR spectrum of naked ZnO

Energy Gap (Eg) of K-ZnO Photocatalyst

The experimental determination of energy gap (Eg) from the reflectance mode of Perkin Elmer Lambda 35 Uv-Vis spectroscopy, was estimated by first converting diffused reflectance spectra to remission function F(R) using Kubelka-Munk expression (eqn2) (Gaya 2011).

$$\frac{k}{s} = \frac{(1-\mathrm{R})^2}{2R} = \mathrm{F(R)} \ldots\ldots\ldots\ldots\ldots\ldots\ldots\ldots\ldots\ldots\ldots\ldots\ldots\ldots\ldots\ldots. (2)$$

Where k and s are the scattering and absorption coefficient respectively, and F(R) is the Kubelka-Munk or remission function and is interchange by k/s. The absorption coefficient k of the direct band gap semiconductor is related to the Tauc equation.

$$\mathrm{k}hv = C_1\left[hv - \mathrm{E_g}\right]^{n} \ldots\ldots\ldots\ldots\ldots\ldots\ldots\ldots\ldots\ldots\ldots\ldots\ldots\ldots\ldots\ldots\ldots\ldots.. (3)$$

Where C_1 is constant, E_g is the average band gap energy of the materials and n value depending on type of the transition for n = ½ E_g in equation (3) is directly allowed band gap.

Then,

$$\mathrm{k}hv = C_1\left[hv - \mathrm{E_g}\right]^{1/2} \ldots\ldots\ldots\ldots\ldots\ldots\ldots\ldots\ldots\ldots\ldots\ldots\ldots\ldots\ldots\ldots\ldots (4)$$

Assuming the optical transition is direct, In this case, by considering the Kubelka-Munk scattering coefficient *s* as constant with respect to wavelength, and using the remission function in equation 4 we obtained the expression:

$[F(R)hv]^2 = C_2\,[hv\text{-}E_g]$……………………………….………………..(5)

The average Tauc band gap energy can be obtained from plot of the intercept of linear portion of the $[F(R)hv]^2$ against *hv*, the K-ZnO band gap was obtained to be 3.28ev Figure 4 (Morales *et al.*, 2007).

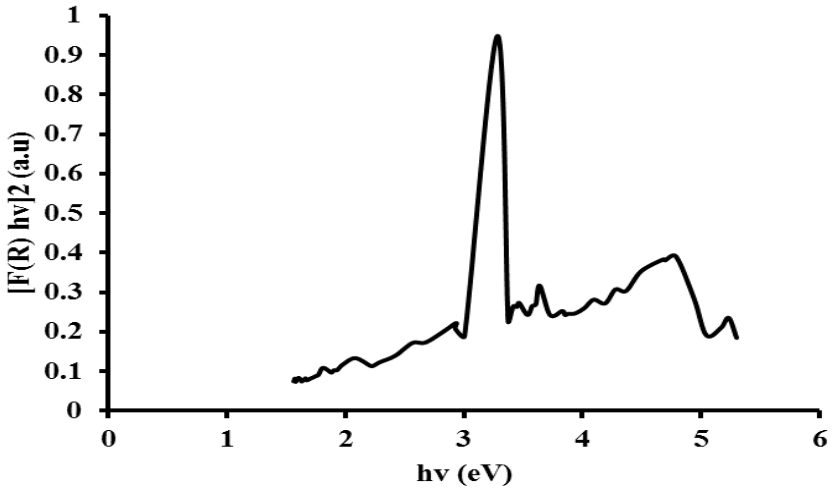

Fig**.** 4**:** Plot of $[F(R)hv]^2$ against photon energy (hv) for K-ZnO photocatalyst.

The Effect of pH

The influence of change in value of pH for the MR degradation is among the most important operating parameter in photocatalytic wastewater degradation process, the value of pH have some effect on properties of the catalyst, figure 5 showed the effect of pH value (4 - 12) of doped and undoped ZnO catalyst. The result indicated that the pH value has significantly influenced the degradation of MR. The percentage degradation of K-ZnO show increase with increase in pH (4 - 8) from 76% to 91% and decreases with increase in pH (10 - 12) 63% to 51% while the percentage degradation of undoped ZnO increases with increase in pH (4 - 10) from 63% to 85% and decreases at pH 12 to 42%. This is due to the potassium precipitate as zinc oxide at higher pH, which resulted in a reduction in the ·OH radical Production and transmission of the radiation (Chen *et al.*, 2007).

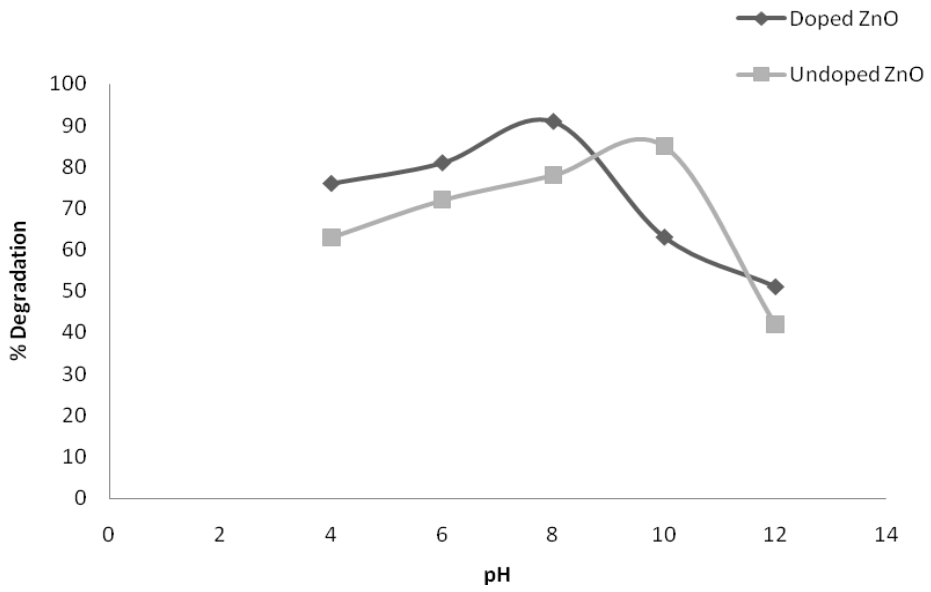

Fig. 5: Percentage degradation of MR, at MR concentration (2ppm), KZnO (0.6g/l), and undoped ZnO (0.6g/l) at 35^{o}C using different pH values.

Effect of Catalyst Dosages

To determine the effect of the doped and undoped ZnO loadings, the catalyst concentration was varied from 0.1 to 1.0 g/dm^3. The percentage degradation of MR increased from 0.1 to 0.6 g/dm^3 and decrease from 0.8 – 1.0g/dm^3 (Figure 6). The decrease in degradation efficiency, at higher catalyst loading levels may be attributed to light scattering by the catalyst particle which attenuates light absorption by the photocatalyst (Ibrahim and Gaya, 2020). The higher degradation rate 95% and 91% was observed with 0.6g/l of the catalyst respectively**.** Hence, catalyst concentration 0.6g/l can be used as an optimum concentration.

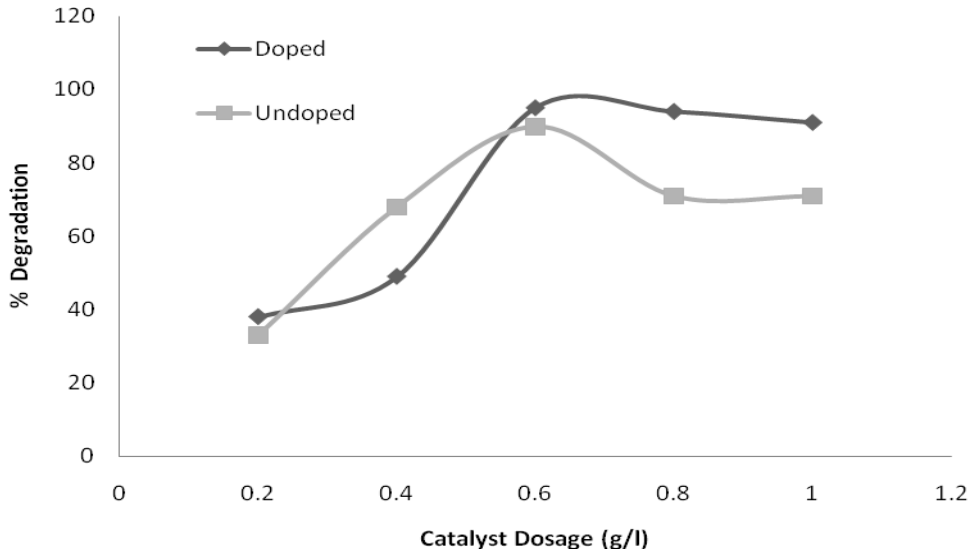

Fig. 6: Percentage degradation of MR at concentration (2ppm), pH value 8 at different K-ZnO and ZnO concentration.

Effect of initial MR concentration

The trend of the degradation of MR dye under visible light illumination was determined (Figure 7). The concentration of MR shows decrease in percentage degradation with increase in MR concentration from 2 – 10 ppm for both doped and undoped catalyst. The increase of MR concentration results from the production of more inorganic ions product like nitrate, chloride and sulfate ions thereby acting as hydroxyl radical scavengers to compete with MR molecule thus, leads to the scarcity of hydroxyl radical which may lead to slow the reaction (Jia *et al.*, 2016).

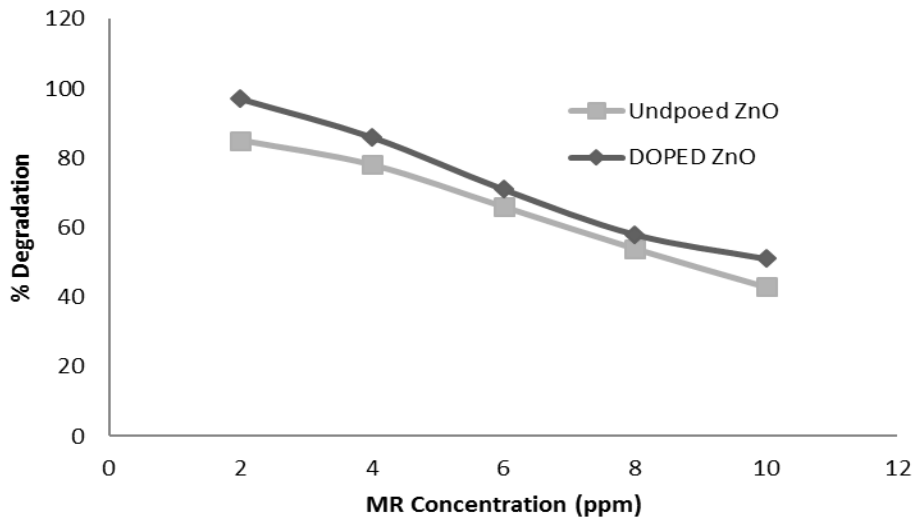

Fig. 7: Percentage degradation of MR at different MR concentration at K-ZnO (0.6g/l), ZnO (0.6g/l) pH value 8 and Temperature 35°C.

KINETICS STUDY

The kinetic for the degradation of MR was tested using pseudo first order and pseudo second order integrated laws expressed by equation (6) and (7). The correlation coefficient (R^2) value and rate constant were calculated from the slope of the graph and summarized in table 1.

$$\ln C_t = -k_1 t + \ln C_o \quad \text{..... (6)}$$

$$\frac{1}{C_t} = k_2 t + \frac{1}{C_o} \quad \text{..... (7)}$$

Where, Co is the initial MR concentration and C_t concentration of MR after time t, k_1 and k_2 are the reaction rate constant of the corresponding orders.

Table.1: Kinetic parameters of K-ZnO and ZnO photocatalytic reaction

Catalyst	Pseudo first		Pseudo second order	
	k (Min^{-1})	R^2	k ($Lmol^{-1}Min^{-1}$)	R^2
Doped ZnO	0.026	0.985	0.065	0.886
Undoped ZnO	0.062	0.922	0.058	0.881

Effect of Temperature on the Reaction Kinetic of K-ZnO

Temperature is critical to the kinetics reaction rate constant K_{MR} for the degradation of MR, a series of experiment were conducted by varying the temperature from 25°C to 55°C with other condition at K-ZnO dosage = 0.8g/dm^3, pH of 8, dye concentration of 2mg/dm^3, at 410nm wavelength the reaction completed in 60 min. with a clear indication that the degradation was accelerated by a rise in temperature (Figure 8). This is due to the higher temperature increase the reaction rate between the K-ZnO and any other form of MR, thus increasing the rate of generation of oxidizing species such as ·OH (Chithambararaj *et al.*, 2013).

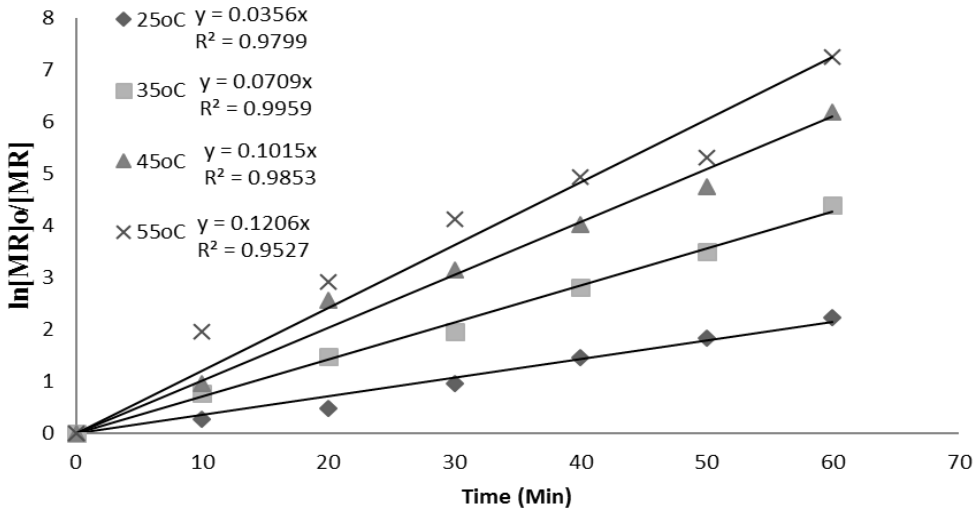

Fig. 8: Plot of ln([MR]$_o$/[MR]) against time as a function of Temperature.

The Arrhenius equation provides a means of determining the value of Ea and A from the measurement of the rate constant at different temperature. The rate of reaction K_{MR} related to temperature (T) and collision parameters by Arrhenius equation.

$$k = \mathrm{Aexp}\left(\frac{-\mathrm{Ea}}{\mathrm{RT}}\right) \quad \text{..... (8)}$$

Where Ea is the apparent activation energy in Jk^{-1}, A is frequency (or pre-exponential) factor, R is gas constant ($8.31JK^{-1}mol^{-1}$) and T is the absolute temperature in kelvin. In this study the variation of the frequency factor and energy of activation of the Arrhenius expression of the degradation of MR may be neglected, this is due to the narrow temperature applied i.e. (25 – 55^{o}C). A linear plot of $\ln k_{MR} = f(1/T)$ are plotted in Figure 9. Good linear relationship exists between the $\ln k_{MR}$ and 1/T, because the correlation coefficient R>>0.9 from Figure 9 based on the Arrhenius equation, the slope –Ea/R and intercept (lnA) are determined (i.e. Ea = 32.109 x 10^3JK^{-1} and A = 1.6 x 10^4min^{-1}).

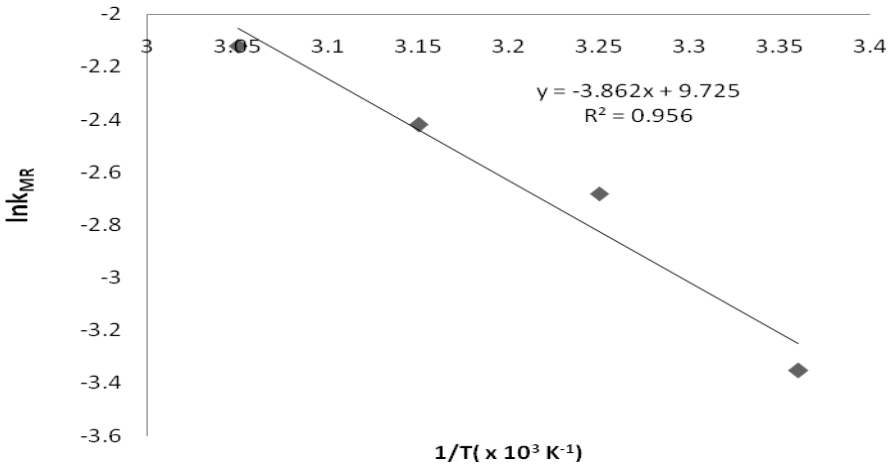

Fig. 9: plot of $\ln k_{MR}$ against 1/T for the MR degradation. Reaction conditions: K-ZnO dosage = $0.8g/dm^3$, pH of 8, [MR] = $2mg/dm^3$, at 410nm wavelength the reaction completed in 60 min.

CONCLUSION

The prepared K-ZnO photo catalyst exhibited excellent photo catalytic efficiency than pure ZnO catalyst over MR degradation using visible irradiation (300w Halogen tube). The K-ZnO greatly facilitates the separation of photogenerated charge carriers and the surface area of the photocatalyst also increases, thus enhanced the photocatalytic efficiency of the catalyst. The effect of operational parameters, pH (4 - 12), catalyst dosage (0.2 - 1.0g/L), and initial MR concentration (2 - 10ppm), Temperature (25 - 55ºC) at the contact time (60 mins) was investigated to study the effect of the process operating parameters and optimum concentration. The Optimum conditions; pH 4 reaction time 60min, initial MR concentration 2mg/l, temperature at 35ºC and catalyst dosage 0.6g/l for both process, which gave MR degradation efficiency of 95% and 91% respectively for doped and undoped ZnO catalysts. The kinetic of both K-ZnO and ZnO followed pseudo first order with correlation coefficient (R^2) value of 0.982 and 0.922 with rate constant of 0.026 min^{-1} and 0.062 min^{-1} respectively.

ACKNOWLEDGMENT

The authors are appreciated the management of the Sule Lamido University, Kafin Hausa for the promoting research and providing financial support in carrying out this investigation.

REFERENCES

Ahmadi, S., Mohammadi, L., Igwegbe, C. A., Rahdar, S., & Banach, A. M. (2018). Application of response surface methodology in the degradation of Reactive Blue 19 using H_2O_2/MgO nanoparticles advanced oxidation process. *International Journal of Industrial Chemistry*, *9*(3), 241–253. https://doi.org/10.1007/s40090-018-0153-4.

Basavarajappa, P. S., Patil, S. B., Ganganagappa, N., Reddy, K. R., Raghu, A. V., & Reddy, C. V.(2020). Recent progress in metal-doped TiO_2, non-metal doped/codoped TiO_2 and TiO_2 nanostructured hybrids for enhanced photocatalysis. *International Journal of Hydrogen Energy*, *45*(13), 7764–7778. https://doi.org/10.1016/j.ijhydene.2019.07.241.

Bechambi, O., Sayadi, S., & Najjar, W. (2015). Photocatalytic degradation of bisphenol A in the presence of C-doped ZnO: Effect of operational parameters and photodegradation mechanism. *Journal of Industrial and Engineering Chemistry*, *32*, 201–210. https://doi.org/10.1016/j.jiec.2015.08.017.

Cheng, X., Li, L., Jia, L., Cai, H., Wang, X., Ding, Y., & Fan, X. (2019). Preparation of K+ doped ZnO nanorods with enhanced photocatalytic performance under visible light. *Journal of Physics D: Applied Physics*, *53*(3), 035301. https://doi.org/10.1088/1361-6463/ab4c17.

Chen, L. C., Huang, C. M., & Tsai, F. R. (2007). Characterization and photocatalytic activity of K+doped TiO_2 photocatalysts. *Journal of Molecular Catalysis A: Chemical*, *265*(1–2), 133–140. https://doi.org/10.1016/j.molcata.2006.10.011.

Chithambararaj, A., Sanjini, N. S., Velmathi, S., & Chandra Bose, A. (2013). Preparation of h-MoO_3 and α-MoO_3 nanocrystals: Comparative study on photocatalytic degradation of methylene blue under visible light irradiation. *Physical Chemistry Chemical Physics*, *15*(35), 14761–14769. https://doi.org/10.1039/c3cp51796a.

Das, A., & Mishra, S. (2017). Removal of textile dye reactive green-19 using bacterial consortium: Process optimization using response surface methodology and kinetics study. *Journal of Environmental Chemical Engineering*, *5*(1), 612–627. https://doi.org/10.1016/j.jece.2016.10.005.

Egea-Corbacho, A., Gutiérrez, S., & Quiroga, J. M. (2019). Removal of emerging contaminants from wastewater through pilot plants using intermittent sand/coke filters for its subsequent reuse.*Science of the Total Environment*, *646*, 1232–1240. https://doi.org/10.1016/j.scitotenv.2018.07.399

Gaya, U. I. (2011). Comparative analysis of ZnO-catalyzed photo-oxidation of p-chlorophenols. *Europian Journal of Chemistry* 2(2), 163–168. https://doi.org/10.5155/eurjchem.2.2.163.

Gaya, U. I., Abdullah, A. H., Zainal, Z., & Hussein, M. Z. (2009). Photocatalytic treatment of 4chlorophenol in aqueous ZnO suspensions: Intermediates, influence of dosage and inorganic anions. *Journal of Hazardous Materials*, *168*(1), 57–63. https://doi.org/10.1016/j.jhazmat.2009.01.130.

Ibrahim, Y., & Gaya, U. I. (2020). Comparative optimization of removal of low levels of Brilliant Green by ZnO photocatalysis and photo-Fenton. *J. Mater.Environ. Sci., 2020 11(2) 318-332*, *11*(2), 318–332. http://www.jmaterenvironsci.com.

Jia, Z., Miao, J., Lu, H. B., Habibi, D., Zhang, W. C., & Zhang, L. C. (2016). Photocatalytic degradation and absorption kinetics of cibacron brilliant yellow 3G-P by nanosized ZnO catalyst under simulated solar light. *Journal of the Taiwan Institute of Chemical Engineers*, *60*(June 2018), 267–274. https://doi.org/10.1016/j.jtice.2015.10.012.

Jiang, M., Ye, K., Deng, J., Lin, J., Ye, W., Zhao, S., & Van Der Bruggen, B. (2018). Conventional Ultrafiltration As Effective Strategy for Dye/Salt Fractionation in Textile Wastewater Treatment. *Environmental Science and Technology*, *52*(18), 10698–10708. https://doi.org/10.1021/acs.est.8b02984.

Liu, B., Lin, L., Yu, D., Sun, J., Zhu, Z., Gao, P., & Wang, W. (2018). Construction of fiber-based $BiVO_4$/SiO_2/reduced graphene oxide (RGO) with efficient visible light photocatalytic activity. *Cellulose*, *25*(2), 1089–1101. https://doi.org/10.1007/s10570-017-1628-8.

Morales E.A., Sanchez Mora E., and Pal U (2007) Use of diffuse reflectance spectroscopy for optical characterization of un-supported nanostructures. *REVISTA MEXICANA DE F´ISICA S* 53 (5) 18–22

Omotunde, O. I., Okoronkwo, A. E., Aiyesanmi, A. F., &Gurgur, E. (2018). Photocatalytic behavior of mixed oxide NiO/PdO nanoparticles toward degradation of methyl red in water. *Journal of Photochemistry and Photobiology A: Chemistry*, *365*(August), 145–150. https://doi.org/10.1016/j.jphotochem.2018.08.005.

Prince Richard, J., KartharinalPunithavathy, I., Johnson Jeyakumar, S., Jothibas, M., & Praveen, P. (2017). Effect of morphology in the photocatalytic degradation of methyl violet dye using ZnO nanorods. *Journal of Materials Science: Materials in Electronics*, *28*(5), 4025–4034. https://doi.org/10.1007/s10854-016-6016-x.

Tominaga, F. K., Dos Santos Batista, A. P., Silva Costa Teixeira, A. C., &Borrely, S. I. (2018). Degradation of diclofenac by electron beam irradiaton: Toxicitiy removal, by-products identification and effect of another pharmaceutical compound. *Journal of Environmental Chemical Engineering*, *6*(4), 4605–4611. https://doi.org/10.1016/j.jece.2018.06.065.

Wang, Y., Jiang, F., Chen, J., Sun, X., Xian, T., & Yang, H. (2020). In situ construction of CNT/cus hybrids and their application in photodegradation for removing organic dyes. *Nanomaterials*, *10*(1). **https://doi.org/10.3390/nano10010178**

Yu, C., Tong, Z., Li, S., & Yin, Y. (2019). Enhancing the photocatalytic activity of ZnO by using tourmaline. *Materials Letters*, *240*, 161–164.https://doi.org/10.1016/j.matlet.2018.12.109.

Zaheer, Z., AL-Asfar, A., &Aazam, E. S. (2019). Adsorption of methyl red on biogenic Ag@Fe nanocomposite adsorbent: Isotherms, kinetics and mechanisms. *Journal of Molecular Liquids*, *283*(March), 287–298. https://doi.org/10.1016/j.molliq.2019.03.030.